J Neurophysiol 111: 918–929, 2014.
First published December 4, 2013; doi:10.1152/jn.00527.2013.

Ongoing activity in the optic tectum is correlated on a trial-by-trial basis with the pupil dilation response

Shai Netser, Arkadeb Dutta, and Yoram Gutfreund
Department of Physiology and Biophysics, The Ruth and Bruce Rappaport Faculty of Medicine and Research Institute, Technion, Haifa, Israel

Submitted 22 July 2013; accepted in final form 1 December 2013

Netser S, Dutta A, Gutfreund Y. Ongoing activity in the optic tectum is correlated on a trial-by-trial basis with the pupil dilation response. *J Neurophysiol* 111: 918–929, 2014. First published December 4, 2013; doi:10.1152/jn.00527.2013.—The selection of the appropriate stimulus to induce an orienting response is a basic task thought to be partly achieved by tectal circuitry. Here we addressed the relationship between neural activity in the optic tectum (OT) and orienting behavioral responses. We recorded multiunit activity in the intermediate/deep layers of the OT of the barn owl simultaneously with pupil dilation responses (PDR, a well-known orienting response common to birds and mammals). A trial-by-trial analysis of the responses revealed that the PDR generally did not correlate with the evoked neural responses but significantly correlated with the rate of ongoing neural activity measured shortly before the stimulus. Following this finding, we characterized ongoing activity in the OT and showed that in the intermediate/deep layers it tended to fluctuate spontaneously. It is characterized by short periods of high ongoing activity during which the probability of a PDR to an auditory stimulus inside the receptive field is increased. These high-ongoing activity periods were correlated with increase in the power of gamma band local field potential oscillations. Through dual recordings, we showed that the correlation coefficients of ongoing activity decreased as a function of distance between recording sites in the tectal map. Significant correlations were also found between recording sites in the OT and the forebrain entopallium. Our results suggest that an increase of ongoing activity in the OT reflects an internal state during which coupling between sensory stimulation and behavioral responses increases.

barn owls; superior colliculus; auditory stimulation; orienting response; habituation

PERIPHERAL SENSORY SYSTEMS are constantly bombarded with stimuli, only a fraction of which induce behavioral responses. A challenge is to understand which stimulus will be selected for behavioral outcome. The "orienting response" is a term coined by Pavlov to include a series of autonomic responses to salient stimuli that prepare the body for action (Sokolov 1963). These include galvanic responses (Bradley 2009), changes in heart rate (Bradley 2009), changes in brain wave activity (Naatanen 1995), and pupillary dilation (Bala and Takahashi 2000). The orienting response, which is remarkably preserved phylogenetically, has served as a long-standing model for studying questions relating to sensory gating and stimulus selection (Barry 2009; Bradley 2009). Salient stimuli such as unexpected events or stimuli that break the regularity of the background are more likely to induce orienting responses, whereas stimuli that are presented repetitively induce habituation (Rankin et al. 2009; Thompson and Spencer 1966).

It has been suggested in numerous studies that the superior colliculus (SC) plays a role in the selection of stimuli (reviews in Boehnke and Munoz 2008 and Knudsen 2007). The SC is, arguably, one of the most phylogenetically conservative structures in the brain (Gaither and Stein 1979; Luksch 2003; Shimizu and Karten 1993). The avian homolog of the SC is the optic tectum (OT). Both mammalian and avian structures share many similarities in their input and output connections (Shimizu and Bowers 1999), and both have been shown to be involved in orienting to salient stimuli (du Lac and Knudsen 1990; Masino and Knudsen 1990; McPeek and Keller 2004; Netser et al. 2010; Wagner 1993) and in multisensory processing (Stein and Meredith 1993; Zahar et al. 2009). An emerging hypothesis is that the evolutionary role of the OT/SC is to sort stimuli based on saliency and send this information to the appropriate brain regions to direct orienting movements, attention, and autonomic responses.

Consistent with the above-mentioned hypothesis, it was found that neurons in the intermediate/deep layers of the OT of the barn owl adapt to stimuli in a manner similar to the habituation pattern of orienting responses (Netser et al. 2011). Moreover, microstimulation in the OT/SC of barn owls and primates induces pupil dilations (Netser et al. 2010; Wang et al. 2012), a classical orienting reflex across species (Bala et al. 2007; Bala and Takahashi 2000; Weinberger et al. 1975).

Here we recorded neural responses in the intermediate/deep layers of the OT simultaneously with pupil dilation responses (PDR). We presented long sequences of auditory stimuli and correlated the fluctuations of the habituated PDR with the neural activity on a trial-by-trial basis. The main finding was that the PDR correlated with the ongoing activity prior to stimulus presentation. We further characterized ongoing activity at the multiunit, single-unit, and local field potential (LFP) levels and report that it is highly variable and characterized by spontaneous episodes of high activity. Using dual recordings, we showed that these episodes were correlated between the OT and the entopallium, the forebrain recipient of the tectofugal pathway (Benowitz and Karten 1976; Reches and Gutfreund 2009). The results of this report demonstrate that ongoing activity in the OT can predict orienting responses. Ongoing activity predicting perception and behavior is reminiscent of findings in cortical areas (Arieli et al. 1996; Fox et al. 2007) but, to the best of our knowledge, has not been reported in the SC or OT.

Address for reprint requests and other correspondence: Y. Gutfreund, Dept. of Physiology and Biophysics, Rappaport Faculty of Medicine, Technion-Israel Inst. of Technology, Haifa 31096, Israel (e-mail: yoramg@tx.technion.ac.il).

MATERIALS AND METHODS

Animals. We used 10 barn owls (*Tyto alba*). All of the birds hatched in captivity. They were kept in large aviaries and were treated in accordance with the guidelines of the Technion Institutional Animal Care and Use Committee. All procedures were reviewed and approved by the Technion Institutional Animal Care and Use Committee.

Electrophysiological recordings. The birds were prepared for repeated experiments in a single surgical procedure: they were anesthetized with 2% isoflurane in a mixture of nitrous oxide (N_2O) and oxygen (4:5). A craniotomy was performed, and a recording chamber was cemented to the skull. At the beginning of each electrophysiological session, the owl was anesthetized briefly with isoflurane (2%) and N_2O in oxygen (4:5). Once anesthetized, the animal was positioned in a custom-made stereotaxic apparatus at the center of a sound-attenuating booth lined with acoustic foam to suppress echoes. The head was fixed to the apparatus and aligned using the pecten oculus—a retinal landmark (Wathey and Pettigrew 1989). Isoflurane was removed within the booth, and the bird was maintained on a fixed mixture of N_2O and oxygen (4:5). The craniotomy cover was removed, and one or two electrodes were driven into the recording chamber with motorized manipulators. The electrodes were platinum-iridium epoxy-coated electrodes or tungsten glass-coated electrodes (~0.5–1.0 MΩ). The electrodes were driven into the different nuclei according to stereotaxic coordinates and physiological characteristics (see below). An online spike sorter (MSD, Alpha-Omega, Nazareth, Israel) was used to isolate single-unit or multiunit action potentials. In several experiments continuous recordings were saved for off-line analysis with AlphaLab SnR (Alpha-Omega). The raw data were filtered and resampled to obtain the LFP signal (0.13–179 Hz, sampling rate 1.39 kHz) and the spike signal (268–8,036 Hz, sampling rate 22.3 kHz). The LFP and spike signals were further analyzed with custom-written MATLAB scripts. At the end of each recording session, the recording chamber was treated with chloramphenicol ointment (5%) and closed. The owl was then returned to its home flying cage.

Auditory stimulation. Computer-generated signals were transduced by a pair of matched miniature earphones (Knowles ED-1914) that were placed at the center of the ear canal ~8 mm from the tympanic membrane. The amplitude and phase spectra of the earphones were equalized within ±2 dB and ±2 μs between 2 and 12 kHz by computer adjustment of the stimulus waveform. Sound levels were controlled by two independent attenuators (TDT PA5) and were set to 13–35 dB SPL.

To assess the auditory receptive fields (RFs) of the recording sites, tuning curves of interaural time differences (ITDs, representing the horizontal position of the sound location) were generated by presenting a series of 100-ms-duration, broadband (3–10 kHz) sounds at an interstimulus interval (ISI) of 1 s with different ITDs. All other acoustic parameters were maintained constant. The ITD value was varied randomly in stimulus sets that were repeated 10–20 times with an ISI of 1 s. The best ITD was defined as the midpoint of the range over which responses were >50% of the maximal response. Curves of the interaural level difference (ILD, representing the vertical position of the sound location) were generated with the same procedure but varying the ILD of the sound.

For inducing pupil responses and evoked neural responses, broadband acoustic stimuli (3–10 kHz) with a duration of 400 ms and a rise/fall time of 5 ms were used. The ITD and ILD of the sounds were adjusted in accordance with the best ITD and best ILD of the recorded site in the OT.

Targeting of nuclei. Identification of the recording site location was based on stereotaxic coordinates and on the anticipated physiological properties of each nucleus: the OT was recognized by characteristic bursting activity and spatially restricted visual and auditory RFs. The position of the recording site within the OT was determined based on the location of the visual RF. Visual RFs were assessed by manually projecting an ophthalmoscope beam on a calibrated screen 1.5 m away from the owl and listening to the recorded spike activity. Once the superficial bursty layer of the OT was reached, the electrodes were lowered further (500–1,000 mm) to tectal layers with reduced bursty activity and regular firing patterns (see Fig. 1 in Netser et al. 2010). These layers corresponded with tectal layers 11–14 (Knudsen 1982; Netser et al. 2010) and together are called intermediate/deep layers. The thalamic auditory nucleus, nucleus ovoidalis (nOv), was targeted 1.0 mm rostral and 5.0 mm medial from the tectal representation of 0° azimuth and 0° elevation relative to the visual axes. In nOv, we searched for robust auditory responses to binaural stimulation, high levels of spontaneous activity, and tonotopic mapping (Perez and Pena 2006). In a previous study (Netser et al. 2011), lesion experiments verified that these coordinates and characteristic firing corresponded with the nOv core. The entopallium was targeted 2 mm rostral, 0.4 mm lateral, and 6.5–7 mm dorsal from the same tectal reference point. In the entopallium, we recorded in the area in which we had previously identified auditory responses (Netser et al. 2011; Reches et al. 2010). This region was characterized by spontaneous bursty activity and strong responses to moving visual stimuli. In all nuclei, the electrode was advanced within the nucleus in 300-μm steps; at each step, basic auditory responses (frequency, ITD, ILD) and/or visual responsiveness were measured first to ensure that the recording site was within the desired nucleus. All recording sites characterized to be within the nucleus were included in the analysis. No post hoc selection of recording sites was performed.

Measuring pupil responses. Pupil responses were measured as described in detail in Netser et al. (2010). Briefly, the owls' right eye was kept open by attaching miniature clips to the small feathers on the eyelids. The clips were pulled gently by strings to adjust a sufficient and stable opening of the eyelids. This procedure did not prevent blinking of the nictitating membrane (allowing for spontaneous moisturizing of the eye). A FireWire video camera (Dragonfly express, IEEE-1394, Point Grey, 30 Hz) equipped with a zoom lens (Pentax c-mount TV-lens, 75 mm, F-1:2.8 fitted with ×2 extender) was positioned ~1 m from the owl's head. An infrared (IR) LED was attached to the camera lens as close as possible to the camera axes. The camera and LED positions were adjusted manually at the beginning of each session to capture optimally the IR light reflected from the retina and obtain a high-contrast image of the pupil. Once the camera was positioned in place the door of the booth was closed, and video sequences of the pupil were collected starting 0.5 s before stimulus onset and ending 3 s after it. Video sequences were analyzed off-line. The video sequence was converted into binary images by using a manually set threshold to optimally separate the pupil area (white pixels) from the surround area (black pixels). The number of white pixels as a function of time in the area of interest was then used as a signal reflecting the pupil response. The area of interest was defined manually for each experiment to include a clear portion of the pupil and its edges (see Fig. 2 in Netser et al. 2010).

Data analysis. The evoked neural responses to an auditory stimulus were quantified as the number of spikes during the stimulus presentation minus the number of spikes during the same amount of time immediately before the stimulus onset divided by the time window. The ongoing activity was quantified as the number of spikes in the 1 s before stimulus onset.

To quantify the PDR, we first reduced the pupil response curve to its baseline by subtracting the average signal in the 500 ms before the stimulus from all points. The PDR magnitude was then defined as the area under the response curve during the poststimulus time window (3 s starting at the onset of stimulation).

To evaluate the relationship between PDR and neural activity, we ranked the trials according to the neural activity magnitude. The average PDR of the 20 trials with the largest neural activity was compared to the average PDR of the 20 trials with the lowest neural

activity. A bootstrap method was used to assess the significance of this comparison. Two groups of 20 trials were drawn randomly, and the difference between the average PDRs was calculated. This was repeated 1,000 times to create a bootstrap distribution. The position of the actual difference relative to the bootstrap distribution (number of standard deviations away from the mean) was used to test the null hypothesis that the difference between the PDRs in the 20 trials with the highest neural activity and the PDRs in the 20 trials with the lowest neural activity is zero.

To examine the population responses, first all PDRs in a single experiment were normalized to the maximal response obtained. Then a two-sample *t*-test was used to compare the normalized PDRs of the 20 trials corresponding with high neural activity to the 20 trials corresponding with low neural activity from all experiments. In addition, for display purposes, population pupil response curves were generated by normalizing each average curve (20 trials corresponding with either high or low neural activity) to its maximum, averaging across all experiments.

To assess the correlation between the fluctuations of ongoing activity of pairs of recording sites, dual recordings were performed for a period of 10–20 min without any stimulation. The ongoing activity in a time window of 1 s was measured every 3 s for periods of 500–1,500 s. This resulted in a histogram of spike rates vs. time (fluctuation vector) for each recording site. The correlation was quantified as the correlation coefficient between the two fluctuation vectors (MATLAB function *corrcoef*). For each pair of sites in OT, a spatial distance in tectal map coordinates was estimated in the following way: the site's best ITD and ILD were converted into degrees of azimuth and elevation by dividing the ITD in microseconds by 2.5 to obtain the azimuth and dividing the ILD by 0.33 to obtain the elevation (Olsen et al. 1989). The spatial distance was the geometrical distance between the two estimated locations. The ITD tuning curves in entopallium and nOv were broader than in OT; in addition, tuning curves in nOv were frequency dependent (Perez and Pena 2006; Reches and Gutfreund 2009). We therefore only used best ITDs and ILDs to estimate the degree of spatial matching between pairs of recording sites in OT. The distribution of the correlation coefficients between nOv and OT was compared with the distributions of the correlation coefficients between the entopallium and OT and between OT pairs, using bootstrap statistics to check the hypothesis that the mean of nOv-OT correlations was shifted to lower correlations. One thousand bootstrap distributions were sampled for the nOv-OT pairs, the entopallium-OT, and the OT-OT pairs. For each distribution a normal curve (Gaussian curve) was fitted and its peak position was extracted. Bootstrap distributions of 1,000 differences between the means were extracted. The position of the actual difference relative to the bootstrap distribution (number of standard deviations away from the mean) was used to test the null hypothesis that the difference between the means of the two distributions is zero.

To verify that the correlations were not contaminated by external artifacts or cross talk between channels, in several sites we repeated the above analysis but removed all spikes that appeared simultaneously in both channels ($\pm$0.2 ms). In all cases, this modification did not change the results in any meaningful manner.

To assess the tendency of large fluctuations in the ongoing activity to be clustered in certain time episodes, we calculated the following index, which we call the clustering index (CI): for each site, the cumulative sum of the fluctuation vector normalized by the sum was first obtained. Then the root mean square of the residuals between the cumulative sum curve and the center diagonal line was calculated. The rationale behind this calculation was that the more clustered the data (i.e., high values tend to segregate), the larger the difference from the diagonal line should be. However, the distance from the center diagonal is also affected by the amplitudes of fluctuations in the data. To compare between different data sets, we randomly shuffled the fluctuation vector and repeated the process (i.e., we calculated the root mean square of the residuals between the cumulative sum of the shuffled data and the center diagonal line). Shuffling was repeated 100 times for each site to narrow the standard error of the estimated value. Figure 4*A*, *inset*, shows an example of the cumulative sum curve of the data compared with a curve of the shuffled data. The CI is the root mean square value of the residuals obtained from the real data divided by the average value from the shuffled data. A value of 1 indicates that trials with high ongoing activity are randomly distributed; values larger than 1 indicate that trials of high ongoing activity tend to cluster; and values smaller than 1 indicate that trials with high ongoing activity tend to be separated (see Fig. 4 for examples of fluctuation vectors and corresponding indexes).

To correlate the power of ongoing LFP with the multiunit activity, the LFP signal was low-pass filtered with a 10th-order Butterworth filter (174.4-Hz cutoff edge). In some recordings where an apparent 50-Hz line noise was observed, an additional step of band-stop filtering was introduced (Kaiser window with transition bandwidth of 1 Hz, with attenuation stop of 60 dB and attenuation pass of 0.01 dB). Power spectrum of LFP was calculated with a running time window of 1 s (*spectrogram* function in MATLAB). Multiunit or single-unit activity was binned at the same time window of 1 s to obtain a fluctuation vector. Correlation coefficients were then calculated (*corrcoef* function in MATLAB) between the fluctuation vector and the average power computed from different frequency bands. To ensure that the correlation coefficients were not dominated by filtered spike shapes in the LFP signal (Zanos et al. 2011), we constructed simulated LFP signals by adding to the original LFP signal shuffled spikes from the same recording. We repeated the same filtering and analysis to obtain the correlation coefficients between the simulated LFP power at different frequency bands and the fluctuation vector of the shuffled spikes. In all the simulated cases correlation coefficients were small and nonsignificant.

RESULTS

Trial-by-trial correlations. We recorded multiunit responses in the deep and intermediate layers of the OT simultaneously with pupil responses. A sequence of 105 identical broadband stimuli was presented with an ISI of 12 s. Importantly, the ITD and ILD of the stimuli were set to match the best ITD and ILD measured at the recording site (see MATERIALS AND METHODS). The responses to the first five stimuli in the sequence were omitted from the analysis, as it was already shown that both neural and behavioral responses undergo habituation during the initial presentations of the stimuli (Bala and Takahashi 2000; Netser et al. 2010, 2011). As expected, in the remaining 100 trials the pupil responses were generally weak because of habituation. However, occasionally some fluctuations of the response occurred. This can be seen in the example shown in Fig. 1*A*. Because of such fluctuations, the average PDR was not completely habituated (Fig. 1*C*). To address whether these behavioral fluctuations were correlated with the trial-by-trial fluctuations of the multiunit neural responses, we sorted the trials according to the strength of the evoked neural response, defined as the number of spikes during the stimulus (400 ms after stimulus onset) minus the number of spikes before the stimulus (400 ms before stimulus onset) (Fig. 1*E*). If a trial-by-trial correlation exists between the neural response and the PDR, we expect positive pupil responses to appear more on the left side of the graph, corresponding with trials of larger neural responses. In the example shown, this was not the case; positive PDRs were distributed irrespective of the neural response (Fig. 1*D*). The average PDR of 20 trials that elicited the strongest neural responses was not different significantly (bootstrap, $P > 0.05$) from the average PDR of 20 trials that elicited

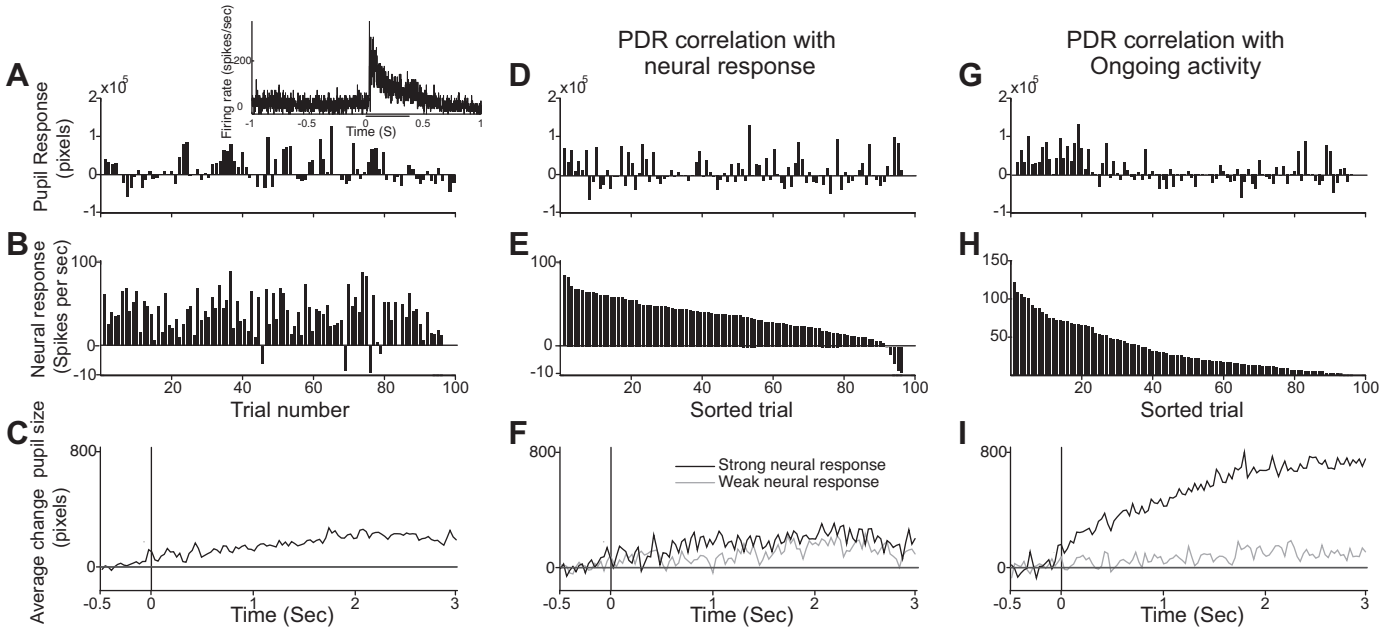

Fig. 1. Trial-by-trial fluctuations of neural and pupil responses from a single recording site in the intermediate/deep layers of the optic tectum (OT). *A*: pupil responses to a sequence of 100 identical stimuli as a function of the position of the stimulus in the sequence. Positive values indicate dilation from rest. *Inset*: average poststimulus time histogram of the multiunit responses to the same stimuli. Horizontal bar indicates stimulus duration. *B*: evoked multiunit responses as a function of the position of the stimulus in the sequence. Responses in *B* were recorded simultaneously with responses in *A*. *C*: average pupil response profile of all trials shown in *A*. Vertical line shows time of stimulus onset. *D*: pupil responses shown in *A*, sorted according to strength of the evoked multiunit response. The trial with the highest neural response is the first, and the trial with the least neural response is the last. *E*: sorted evoked responses. *F*: average pupil response profile of the first 20 sorted trials corresponding with the trials of high evoked neural activity (black curve) overlaps with average pupil response profile of the last 20 sorted trials corresponding with the trials of weak evoked activity (gray curve). *G*: pupil responses shown in *A* sorted according to the level of ongoing multiunit activity. The trial with the highest activity is the first, and the trial with the smallest activity is the last. *H*: sorted ongoing multiunit activity. *I*: average pupil response profile of the first 20 sorted trials corresponding with the trials of high ongoing activity (black curve) overlaps with average pupil response profile of the last 20 sorted trials corresponding with the trials of weak ongoing activity (gray curve).

the lowest neural responses (Fig. 1*F*), suggesting indifference of the PDR with respect to the magnitude of the evoked response in the OT. However, at this recording site, as in many others, the level of ongoing activity, measured as the number of spikes in a time window of 1 s just before the onset of stimulation, varied considerably between trials. Therefore, we performed an additional analysis in which the trials were sorted according to the level of ongoing activity rather than the evoked responses. When the data were sorted in this way, positive PDRs were significantly (bootstrap test, $P < 0.05$) more concentrated on the left side of the graph (Fig. 1, *G* and *H*). The 20 trials with the strongest ongoing activity elicited a stronger average pupil dilation compared with the 20 trials with the lowest ongoing activity (Fig. 1*I*). An additional trial-by-trial analysis was performed to assess correlation between the ongoing activity in the OT and the baseline pupil size (measured prior to stimulation), and no significant correlation was observed (not shown).

The basic result shown in the above example, namely, that the PDR was significantly correlated with the trial-by-trial fluctuations of the ongoing activity and not the response itself, was observed significantly in 9 of 21 recording sites (bootstrap analysis, $P < 0.05$). This observation was also significant at the population level. Figure 2*A* shows the population average pupil response of the 20 trials with the highest ongoing activity from all recording sites in the OT ($n = 21$ in 1 owl) compared with the population average of the 20 trials with the lowest ongoing activity. The average PDR corresponding with high ongoing activity was significantly larger than the average PDR corresponding with low ongoing activity (*t*-test, $P < 0.05$). On the other hand, the evoked response (post − pre) showed a different pattern: the population average PDR corresponding with the largest evoked responses was significantly smaller (*t*-test, $P < 0.05$) than the population average PDR corresponding with the lowest evoked responses (Fig. 2*B*).

The entopallium receives information about salient stimuli from the OT through the tectofugal pathway (Marin et al. 2007; Reches and Gutfreund 2008) and may play a role in mediating orienting responses (Gutfreund 2012). We therefore examined the trial-by-trial correlations between the PDR and activity (evoked and ongoing) recorded in the entopallium. The results from the entopallium were similar to the results from the OT, namely, the ongoing activity in entopallium was correlated with the PDR at the population level ($n = 19$ from 2 owls) (Fig. 2*C*), whereas the evoked neural responses were not (Fig. 2*D*).

Next, we examined whether the trial-by-trial correlation requires matching between the recording site and the stimulus location or is a global phenomenon in the OT. For this purpose, we used two auditory stimuli, one positioned at the best ITD and ILD of the recording site (matched stimulus) and the other at the opposite ITD and ILD (unmatched stimulus). The two stimuli were presented alternately every 12 s (see Fig. 3*A*). As in the previous analysis, the trials were sorted according to the level of ongoing activity, and the 20 responses with the largest activity were averaged and compared to the 20 responses with the lowest activity. This experiment was repeated at 45 recording sites from three owls, and the results were averaged to

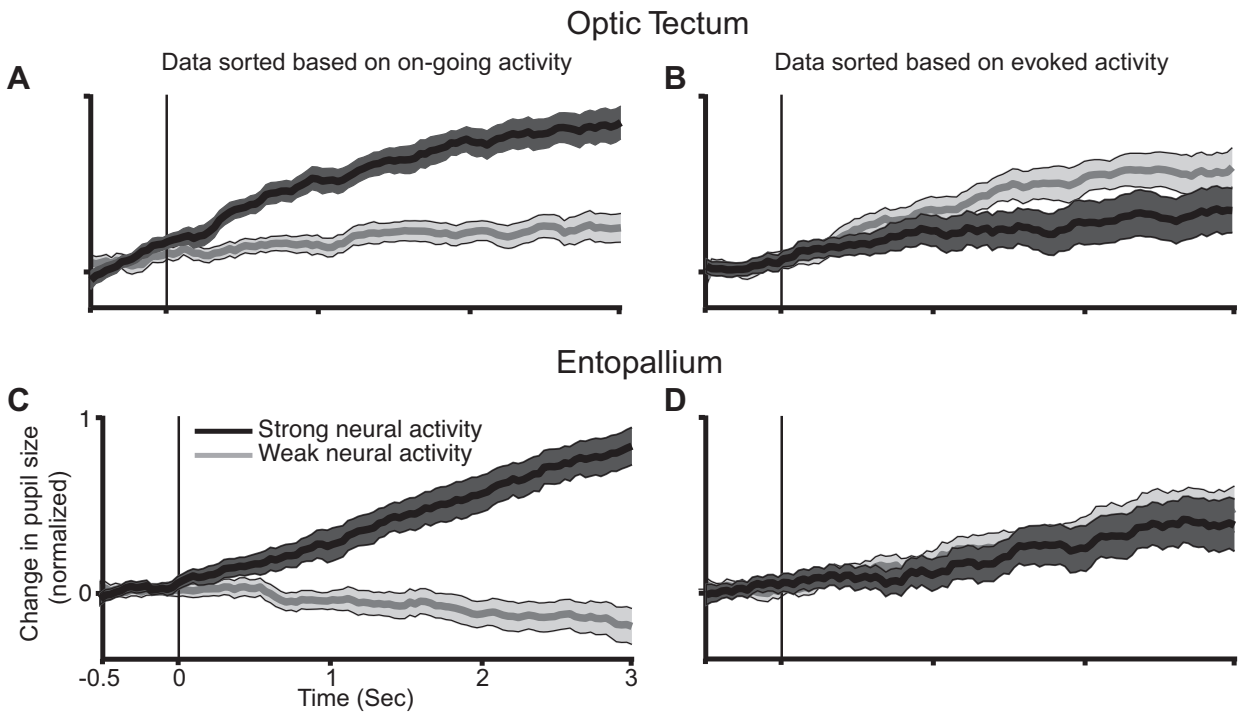

Fig. 2. Comparison of population pupil responses during high and low neural activity in the OT and the entopallium. *A*: population average pupil response profile from the 20 trials of high ongoing activity (black curve) is superimposed onto population average pupil response from the 20 trials of low ongoing activity (gray curve). Width of the curves designates SE. Vertical line designates time of stimulus onset. *B*: population average pupil response profile from the 20 trials of high evoked neural responses (black curve) is superimposed onto population average pupil response from the 20 trials of low evoked neural responses (gray curve). *C*: same as in *A*, but for neural data recorded in the entopallium. *D*: same as in *B*, but for neural data recorded in the entopallium.

obtain the population responses. The population PDR in the trials with high ongoing activity was larger than the PDR with low ongoing activity when the stimulus matched the recording site (Fig. 3*B*). This difference was highly significant (*t*-test, $P < 0.0001$). When the stimulus did not match the recording site, the population PDR in the high ongoing activity trials only slightly exceeded the population PDR in the low ongoing activity, albeit below the significance level of 5% (Fig. 3*C*; *t*-test, $P = 0.046$). Therefore, we conclude that the trial-by-trial correlation between ongoing activity and PDR was stronger for stimuli represented at the recording site compared with stimuli represented elsewhere in the map.

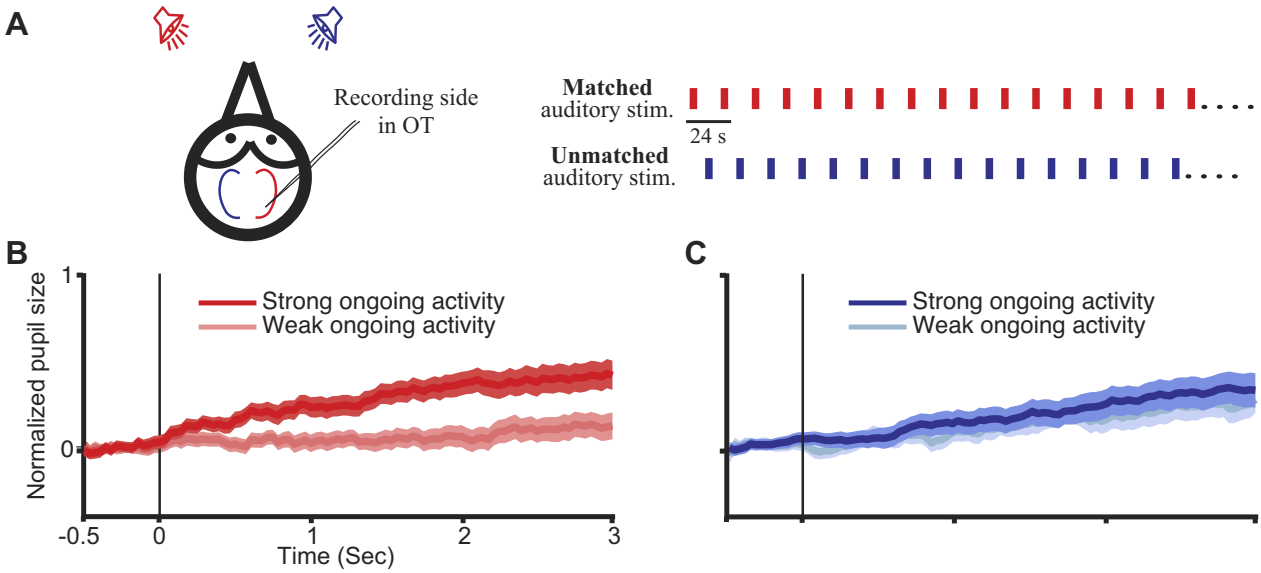

Fig. 3. Correlations between pupil responses and neural activity in matched vs. unmatched recording sites. *A*: diagram showing the stimulation paradigm. Two stimuli were presented in an alternating sequence with an interstimulus interval (ISI) of 12 s. One stimulus (red) matched the best interaural time (ITD) and interaural level (ILD) difference of the recording site, while the other stimulus (blue) did not. *B*: population average pupil response profiles for the matched stimulus. Dark curve shows the average of the 20 trials of high ongoing activity and light curve the average of the 20 trials of low ongoing activity. Width of the curves designates SE. Vertical line designates time of stimulus onset. *C*: population average pupil response profiles for the unmatched stimulus. Format as in *B*.

Ongoing activity. The results of the experiments above suggest that ongoing activity before stimulus onset is functionally significant. Therefore, we next turn to characterize the ongoing activity. Figure 4*A* illustrates the multiunit neural activity measured in a recording site in the OT. The histogram shows the spike rate of the ongoing activity measured at fixed time intervals (3-s separation). Figure 4*A*, *inset*, shows the normalized cumulative sum of the ongoing activity compared with the cumulative sum of the shuffled data. It is apparent that the fluctuations in activity are not distributed randomly; rather, the trials of high ongoing activity tend to cluster. These periods of high ongoing activity tend to continue for several seconds to tens of seconds and appear every few minutes.

To quantify the tendency of a site to show epochs of high ongoing activity, we used the clustering index (CI; see MATERIALS AND METHODS). Two additional examples are shown in Fig. 4, *B* and *C*, one with a high CI and one with a low CI. The CIs in the OT were all above 1 (minimum = 1.29, median = 2.08, maximum = 3.54), indicating that ongoing activity tended to cluster in time. To address whether the tendency of ongoing activity to cluster was related to the trial-by-trial correlation of the ongoing activity with the PDR, we separated the population of recording sites (shown in Fig. 2) into two groups according to the value of their CI. The recording sites with high CIs showed stronger correlations on average between ongoing activity and PDR compared with the recording sites with smaller CIs (Fig. 4, *D* compared with *E*). Therefore, it seems that unexplained periods of high ongoing activity occasionally arise in the OT, and during these periods the pupil response tended to be less habituated.

To address whether the periods of high ongoing activity are local or global, we inserted two electrodes into the OT and measured the correlation coefficient between the multiunit ongoing activities at the two recording sites ($n = 14$ from 2 owls). Figure 5 shows the correlation coefficient as a function of the distance index between the two recording sites (see MATERIALS AND METHODS). A significant negative tendency can be observed: sites with closer RFs tended to show higher correlation coefficients compared with sites with distant RFs ($P < 0.001$, see 2 examples of results from dual recordings in Fig. 5, *insets*). This result demonstrates that the increase in ongoing activity reflects a mostly local effect and not a simultaneous increase in the entire OT.

The next question was whether the ongoing activity could be correlated with recording sites outside the OT. For this purpose, we recorded simultaneously using two electrodes, one in the OT and the other either in the entopallium or in the nOv. The nOv, the main thalamic auditory nucleus, represents a station along the thalmofugal pathway (Perez et al. 2009), whereas the entopallium represents a station along the tectofugal pathway (Reches and Gutfreund 2009). Figure 6 shows two examples of such dual recording sites in the OT and the

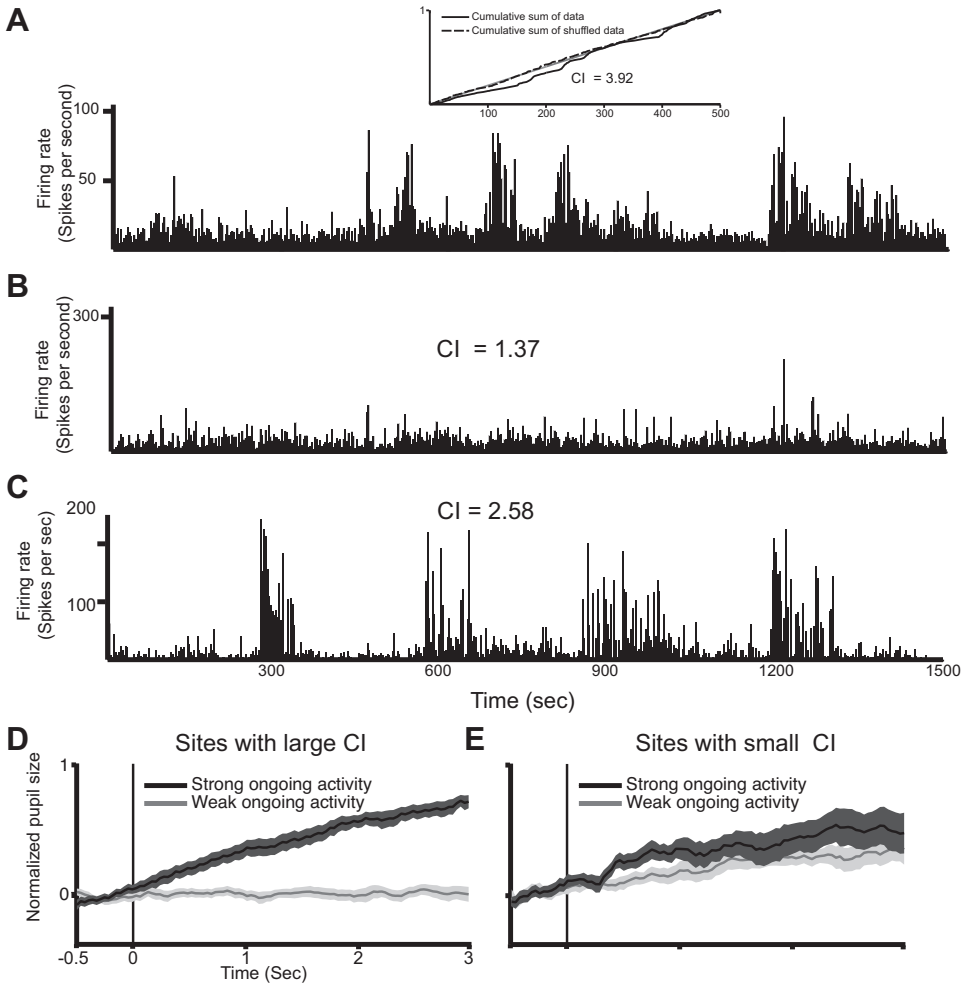

Fig. 4. Trial-by-trial correlations from sites with high fluctuations of ongoing activity vs. sites with low fluctuations. *A*: example of a fluctuation vector of the ongoing activity in 1 tectal site. Each bin represents the ongoing activity measured in a time window of 1 s, with an interwindow interval of 3 s. *Inset*: cumulative sum of the fluctuations compared with cumulative sum of the shuffled data. *B* and *C*: 2 additional examples of fluctuation vectors of ongoing activity: 1 with a low clustering index (CI) value (*B*) and 1 with a high CI value (*C*). *D*: population average pupil response profiles from all experiments in which CI was above the median. Dark curve shows the average over the 20 trials of high ongoing activity and light curve the average over the 20 trials of low ongoing activity. Width of the curves designates SE. Vertical line designates time of stimulus onset. *E*: population average pupil response profiles from all experiments in which CI was below the median. Format as in *D*.

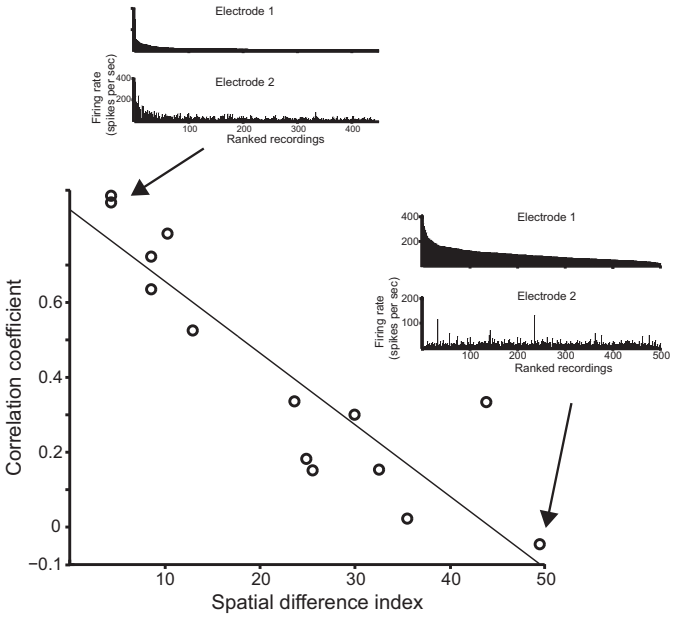

Fig. 5. Dual recordings in the OT. Correlation coefficients between pairs of dual recordings in the OT as a function of the distance between the 2 recording sites. Black line shows the regression line. *Inset* on *left*: levels of ongoing activities from a pair of tectal recordings sorted according to strength of ongoing activity at *electrode 1*. In this case, the electrodes were in close proximity. *Inset* on *right*: example from a different pair of tectal recordings. In this case, the electrodes were located further apart.

entopallium (Fig. 6*A*) and in the OT and the nOv (Fig. 6*B*). The results are sorted according to strength of response in the OT (Fig. 6, *A* and *B*, *top*). A tendency for correlation can be observed with ongoing activity in entopallium (Fig. 6*A*, *bottom*) but not in nOv (Fig. 6*B*, *bottom*). This tendency was quantified by calculating the correlation coefficient between each pair of recordings (see MATERIALS AND METHODS). The distribution of the correlation coefficients between OT and nOv measured from eight dual recording sites from two owls is shown in Fig. 6*C*. The median was not significantly different from zero (sign test, $P > 0.05$; Fig. 6*C*). The median of the distribution of the correlation coefficients between the entopallium and the OT ($n = 10$ from 2 owls) was shifted significantly to positive values (sign test, $P < 0.01$; Fig. 6*D*). These distributions were also compared with the distribution of the correlation coefficients between pairs of recordings in the OT (data from Fig. 5 shown as a distribution histogram in Fig. 6*E*). The Gaussian fits to the three distributions (OT-nOv, OT-entopallium, and OT-OT) are shown in Fig. 6*F*. The population of nOv recording sites were significantly less correlated with tectal sites (bootstrap statistics, $P < 0.01$) compared with the population of recording sites from the entopallium and with recording sites in the OT (Fig. 6*F*). The correlation coefficients from the population of recording sites in the entopallium, on the other hand, were not significantly different from the correlations obtained within the OT (Fig. 6*F*; bootstrap statistics, $P > 0.05$).

In summary, ongoing activity in the OT is unstable, experiencing short periods of high activity. These periods tend to correlate between the OT and the entopallium and between close sites in the OT but are significantly less correlated with activity in the nOv. Moreover, multiunit sites that produced robust periods of high ongoing activity tended to show better correlation with pupil responses.

Correlation between multiunit, single units, and LFP. A similar tendency for clustering of ongoing activity was observed at the single-unit level. Figure 7*A* shows an example of a stable single unit recorded over a period of ~10 min together with the multiunit signal recorded from the same electrode (excluding the single unit). A roughly simultaneous epoch of increase in spike rate can be seen in both signals (correlation coefficient = 0.5, $P < 0.01$). Figure 7*C* shows two stable single units recorded from the same electrode over a period of ~10 min. It can be seen that the two units tended to fluctuate in a synchronized manner (correlation coefficient = 0.2, $P < 0.01$).

Recent studies suggested that the power of induced gamma oscillations in the avian tectum carries information about the stimulus and is related to spatial attention (Marin et al. 2012; Sridharan et al. 2011). It is therefore of interest to characterize fluctuations of the ongoing LFP signal and examine its correlation with the ongoing fluctuations of the multiunit signal. The spectrogram of the simultaneous LFP signal is shown in Fig. 7, *B* and *D*. It can be seen that in both cases increases in the LFP power correspond with increases in spiking activity. Figure 8*A* shows an example from another recording site in the OT recorded for ~8 min without any stimulation. Figure 8*A*, *bottom*, shows the ongoing multiunit spike rate. Figure 8*A*, *top*, shows the normalized LFP power at four frequency bands: 2–10 Hz, 10–20 Hz, 20–90 Hz, and 90–150 Hz, corresponding with theta, beta, low gamma, and high gamma oscillations (Sridharan et al. 2011). In the example shown it can be seen that epochs of high ongoing multiunit activity are mirrored in the low and high gamma band LFP but not in the beta and theta bands. This result can be seen in the population average as well. The blue curve in Fig. 8*B* shows the correlation coefficient as a function of the LFP frequency band averaged across multiple recording sites in the deep/intermediate layers ($n = 9$ from 2 owls). Correlation coefficients tended to increase with the frequency of the LFP. Frequencies at the high gamma band demonstrated the highest correlations between LFP and multiunit signals. The gray curve in Fig. 8*B* shows the result of the same analysis performed for the shuffled data (see MATERIALS AND METHODS). The lack of correlation at all frequencies in the shuffled data indicates that the result described above cannot be attributed to spike contamination of the LFP signal (Zanos et al. 2011).

DISCUSSION

In this study, we report high fluctuations of ongoing activity in the OT. Spontaneous fluctuations in ongoing activity have been reported in a variety of cortical and subcortical areas at all levels of neural recordings from single units to fMRI (Arieli et al. 1996; Boly et al. 2007; Fox and Raichle 2007; Nir et al. 2006). In some cases, the fluctuations of ongoing activity exceeded the evoked response itself (Arieli et al. 1996). This was also the case in several of our recording sites in the OT [see, for example, Fig. 1; the standard deviation of the ongoing activity was 30.19 (spikes/s) whereas the average evoked response was 28.12 (spikes/s)]. Many studies regard variability of ongoing activity as noise and hence eliminate it by reporting the magnitude of the evoked response above the spontaneous

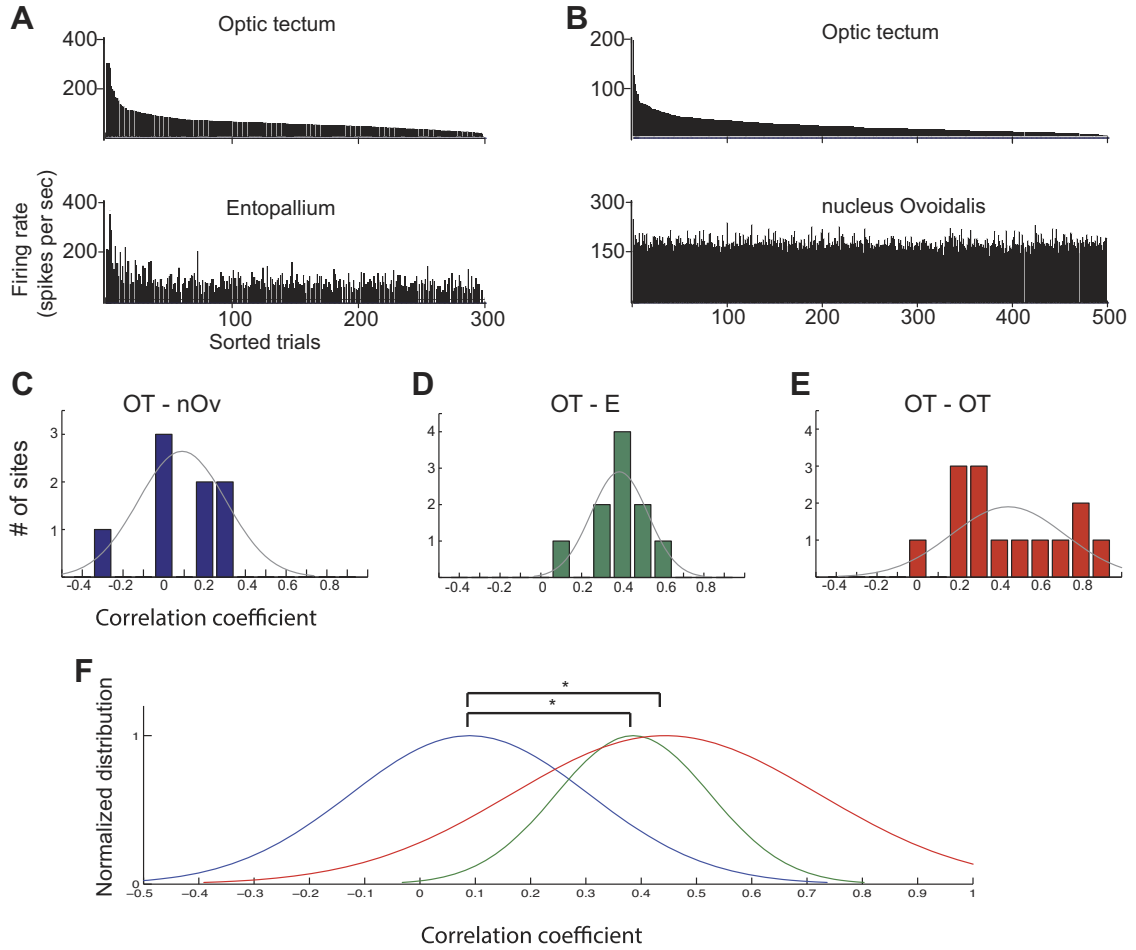

Fig. 6. Dual recordings in the OT and the nucleus ovoidalis (nOv) and in the OT and the entopallium. *A*: example of the results from a pair of simultaneous recorded sites in the OT and the entopallium. *Top*: ongoing activity sampled every 2 s in the OT sorted according to level of activity, the highest level on *left* and the lowest level on *right*. *Bottom*: corresponding ongoing activity measured simultaneously in the entopallium. *B*: example of the results from a pair of simultaneously recorded sites in the OT and the nOv. *Top*: ongoing activity sampled every 2 s in the OT sorted according to level of activity, the highest level on *left* and the lowest level on *right*. *Bottom*: corresponding ongoing activity measured simultaneously in the entopallium. *C*: distribution of correlation coefficients of ongoing fluctuations measured in a population of dual recordings, 1 in the OT and 1 in the nOv. *D*: distribution of correlation coefficients of ongoing fluctuations measured in a population of dual recordings, 1 in the OT and 1 in the entopallium. *E*: distribution of correlation coefficients of ongoing fluctuations measured in a population of dual recordings, both in the OT. Gray curves in *C–E* are the normal distribution fits of the histogram data. *F*: normalized fitted curves of the normal distributions from *C–E* are shown on a single axis for comparison. Blue curve corresponds with the data in *C*, green curve with the data in *D*, and red curve with the data in *E*. *Significant shift between the means of the 2 distributions (bootstrap statistics, $P < 0.01$).

level or by averaging the ongoing activity across trials. The justification behind this process is the notion that the brain can get rid of the noise by averaging across neurons (Raichle 2006). However, for this the noise must be uncorrelated, a condition that was not satisfied in our recordings. Dual recordings in the OT showed a high degree of ongoing activity correlations between adjacent sites. This is not an uncommon observation: large-range correlations of ongoing activity have been reported in numerous studies (for example, Lampl et al. 1999; Nir et al. 2008; Tsodyks et al. 1999). Moreover, in many cases, large fluctuations in ongoing activity were measured in global signals such as EEG and BOLD (Fox and Raichle 2007; Rodriguez et al. 1999), suggesting a large degree of synchronization between neurons. This raises the alternative hypothesis that ongoing activity is not spontaneous noise but is rather modulated by internal states of the animal, such as awareness levels, attention loads, priorities, and/or expectations (Arieli et al. 1996; Engel and Singer 2001; Fox et al. 2005). The ongoing activity then interacts with incoming sensory signals to shape the behavioral response in a context-dependent manner (Fiser et al. 2004; Fox et al. 2007).

In this study, we used a trial-by-trial analysis to address the relationship between neural activity in the OT and behavioral responses. In a trial-by-trial analysis, we seek a correlation between the variability of the neural response and the variability of the behavior (Shadlen et al. 1996). We found that the variability of ongoing activity measured before stimulus presentation tended to predict the fluctuation of the habituated PDR. This finding is reminiscent of findings in the visual and auditory cortex of primates and humans, which showed that ongoing activity can be correlated with perception (Hesselmann et al. 2008; Sadaghiani et al. 2009; Super et al. 2003). To the best of our knowledge, this is the first study showing that ongoing activity in the optic tectum is correlated with orienting responses. Consequently, we suggest that greater attention should be paid to ongoing activity in the OT or its homolog, the SC.

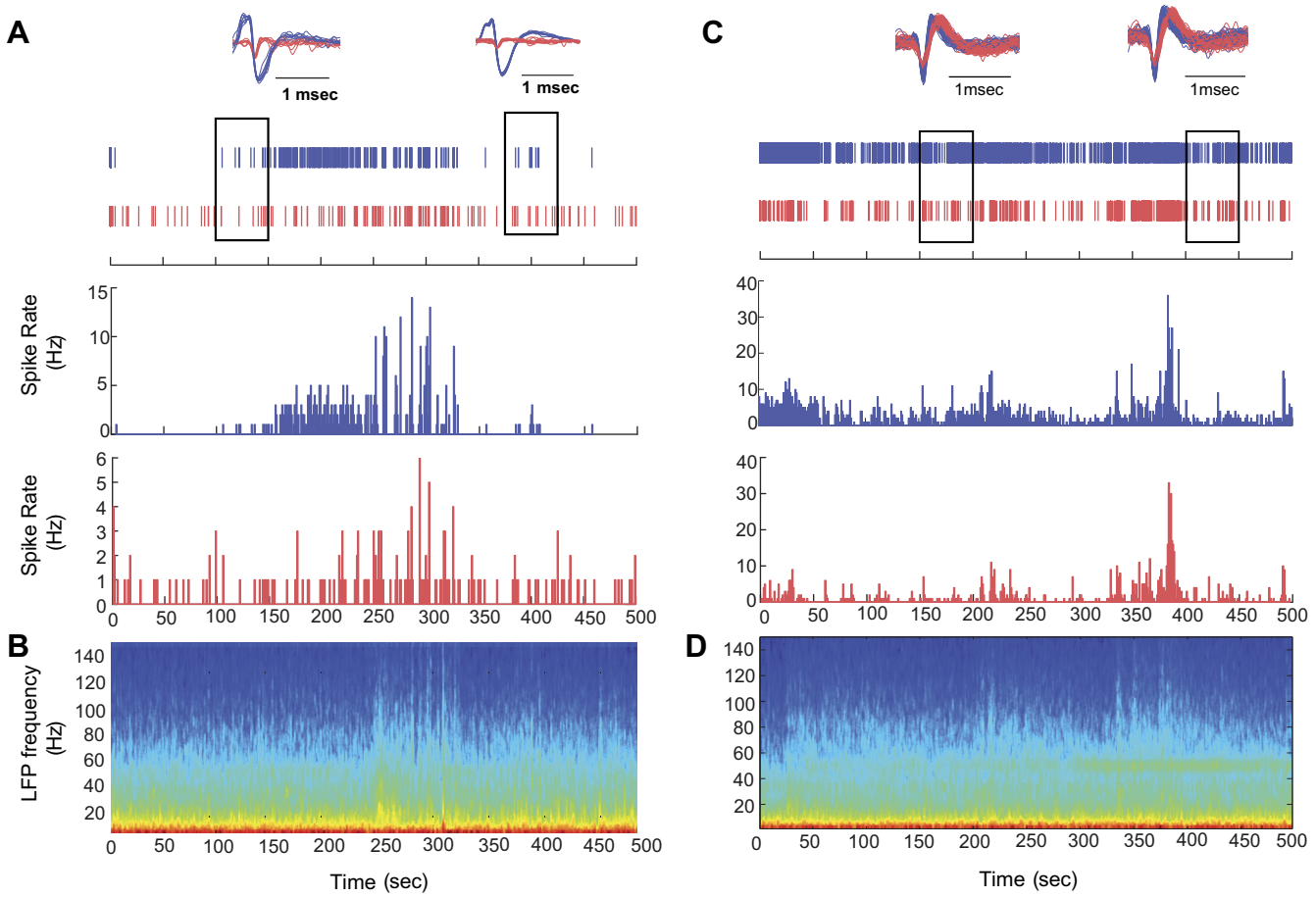

Fig. 7. Example of continuous single-unit recordings. *A*, *top*: rasters of a continuous 500-s recording of a single unit (blue raster) and a simultaneous multiunit signal (excluding the single unit) recorded with the same electrode (red raster). *Insets*: overlapping waveforms of the isolated unit (blue) together with multiunits (red) during the periods marked by squares in the rasters. *Left inset* corresponds with *left* square and *right inset* with *right* square. *Bottom*: graphs show corresponding poststimulus time histograms (time bins of 1 s) of the single unit (blue) and the multiunit (red). *B*: spectrogram of the local field potential (LFP) signal recorded simultaneously with the same electrode as in *A*. Color codes the power of the signal: blue indicates low power and red high power. *C*: example of a continuous recording of 2 single units with 1 electrode. Format as in *A*. *D*: spectrogram of the LFP signal recorded simultaneously with the same electrode as in *C*. Format as in *B*.

A major question then is, What is the source of the variability in tectal ongoing activity? Is it possible that the strong fluctuations are an outcome of the anesthesia state? The animals in this study were sedated with N_2O; hence they may switch spontaneously between wakeful and sedated states. Such spontaneous switches may explain the large fluctuations in ongoing activity and the correlation with behavioral responses. However, the ongoing activity correlated more with PDRs to spatially matching stimuli compared with nonmatching stimuli (see Fig. 3) and was mostly not correlated between the OT and the nOv (see Fig. 6). This locality of the correlations makes it less likely that wakefulness state, which is expected to be a global phenomenon (Huguenard and McCormick 2007), dictates the observed fluctuations. Still, it is a possibility that the large fluctuations are an outcome of the unnatural sedated state, but the mechanism is local. It is yet to be shown whether similar fluctuations of ongoing activity can be recorded in unsedated barn owls.

Many neurons in the OT are constantly inhibited (Felix et al. 1994; Hikosaka et al. 2000). Bicuculline injections into the OT result in a dramatic increase in the level of ongoing activity (Gutfreund et al. 2002). It is therefore a possibility that the fluctuations in ongoing activity that we observe in the OT reflect modulations of inhibitory load. One main inhibition pathway to the OT originates in nucleus isthmi magnocellularis (Felix et al. 1994; Luksch 2003; Mysore and Knudsen 2011). This pathway was suggested to be involved in stimulus selection (Lai et al. 2011; Marin et al. 2012; Mysore et al. 2010; Mysore and Knudsen 2013), and therefore its removal is expected to result in stronger responses to stimuli as well as greater ongoing activity. However, inhibition from nucleus isthmi magnocellularis is global, inhibiting large portions of the OT (Knudsen 2011; Wang et al. 2004), and it therefore cannot explain the locality of the correlation (Fig. 3). An alternative possibility is that the fluctuations reflect a modulation of excitatory pathways to the OT, such as the nucleus isthmi parvocellularis-tectal pathway (Maczko et al. 2006; Wang et al. 2006) or the arcopallio-tectal pathway (Cohen et al. 1998; Knudsen et al. 1995). Both pathways are topographic (Marin et al. 2007; Wang et al. 2006; Winkowski and Knudsen 2007) and can therefore account for the locality of the correlation effect. Moreover, both pathways have been linked with the process of stimulus selection (Asadollahi et al. 2011; Marin et al. 2007, 2012; Winkowski and Knudsen 2006). Future pharmacological experiments should be able to discern between the different possibilities.

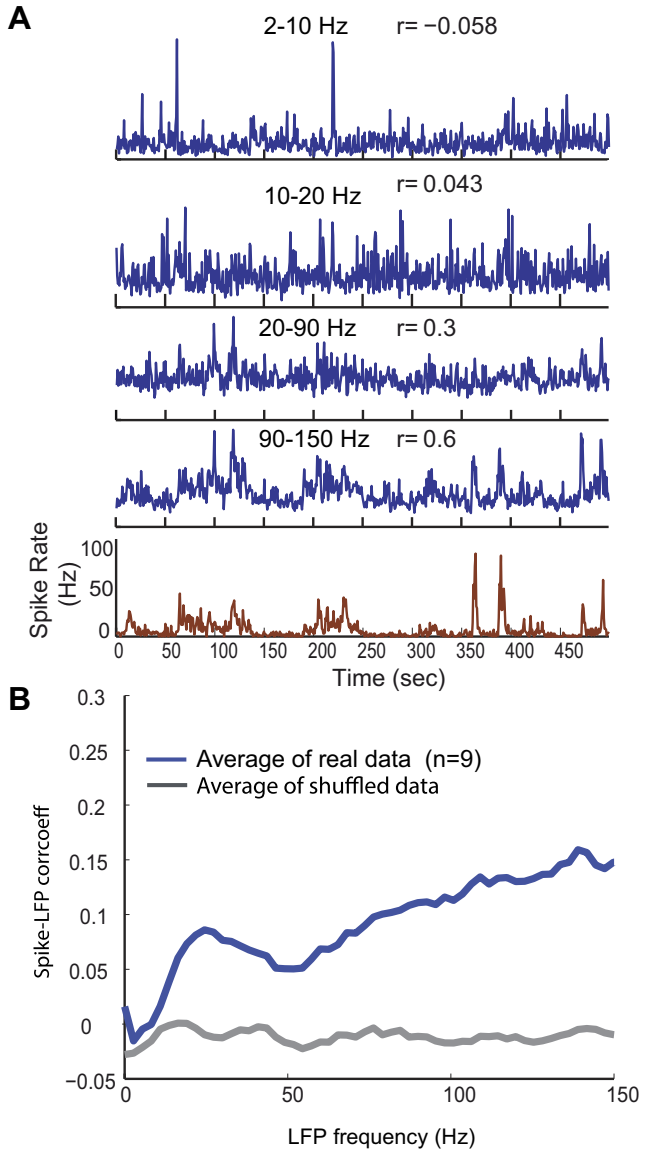

Fig. 8. Correlation between ongoing multiunit activity and LFP. *A*: example of a single recording site in the deep/intermediate layers of the OT. *Bottom*: spike rate as a function of time from onset of recording. Time bins for spike rates are of 1 s. *Top*: average power of the LFP at frequency bands, from *top* to *bottom*, of 2–10 Hz, 10–20 Hz, 20–90 Hz, and 90–150 Hz. *y*-Axes are normalized to the extent of the maximal value in each frequency band. The correlation coefficient value of each frequency band is indicated above each panel. *B*: blue curve shows the average correlation coefficient between the power of the LFP and the multiunit signal as a function of the frequency in a population of recording sites in the deep/intermediate layers of the OT. Gray curve shows results of the same analysis performed with the shuffled multiunit signal.

Although the main result of this report, that ongoing activity in the intermediate/deep layers of the OT is correlated with behavioral responses, has not been shown previously, we argue that to some extent it is an expected result. The OT (as well as its mammalian homolog, the SC) is considered to be a hub in the brain network that coordinates the responses to salient stimuli (Boehnke and Munoz 2008; Fecteau and Munoz 2006; Knudsen 2007). Responses to sensory stimuli in the intermediate/deep layers of the OT are highly context dependent (Frost and Nakayama 1983; Mysore et al. 2010, 2011; Netser et al. 2011; Reches and Gutfreund 2008; Woods and Frost 1977; Zahar et al. 2009). Neurons in these layers express a variety of cholinergic, glutamatergic, and GABAergic receptors (Goddard et al. 2012; Luksch 2003; Sorenson et al. 1989), suggesting a rich background for neural modulations. Studies have reported that priming by microstimulation or sensory stimulation can modulate behavioral and neural responses in the OT (Netser et al. 2010; Winkowski and Knudsen 2007). Moreover, gamma band network oscillations can be recorded in the LFP and in multiunit signals in the OT (Goddard et al. 2012; Neuenschwander et al. 1996; Sridharan et al. 2011). The amplitude of these gamma oscillations has been suggested to relate to internal states such as spatial attention. Therefore, it is likely that internal states modulate neural responses in the intermediate/deep layers of the OT through a rich network of connections from other brain areas (Luksch 2003). Such modulations are likely to affect ongoing activity in the OT as well as behavioral responses.

An intriguing observation in our data was that while ongoing activity before the stimulus tended to correlate with the PDR, the response to the stimulus itself did not. In fact, at the population level, the strength of the evoked response was to a small extent negatively correlated with behavior. This observation may be due to the large fluctuations in ongoing activity causing a ceiling effect on the evoked responses. It is possible that the readout mechanism takes the overall activity (evoked + ongoing) into account. Since the evoked responses are generally habituated and hence small (Netser et al. 2011), the ongoing activity mostly dominates the behavioral responses. This possibility has been suggested to explain correlations between ongoing cortical BOLD and perception (Fox and Raichle 2007). In addition, the information to respond may not be simply coded in the single neuron's evoked response but rather at a population level (Lewis and Lazar 2013).

A recent study in pigeons demonstrated significant cross-correlations between spiking activity in the OT and the entopallium. Moreover, the cross-correlograms between these two structures were dominated by gamma band oscillations (Marin et al. 2012). Here we show that the level of ongoing activity in the OT and the entopallium tends to be correlated and to predict behavioral responses. This result suggests that information about the behavioral response to a stimulus may be found in the correlations of spikes between tectal and entopallial neurons and further supports the notion that the OT and the entopallium work in concert to select and control orienting responses. (Marin et al. 2007, 2012; Gutfreund 2012).

ACKNOWLEDGMENTS

We thank Dr. Omri Barak for helpful discussions about procedures of analysis.

GRANTS

This work was supported by a grant from the Israel Science Foundation and the Langman Research Fellowship for Y. Gutfreund.

DISCLOSURES

No conflicts of interest, financial or otherwise, are declared by the author(s).

AUTHOR CONTRIBUTIONS

Author contributions: S.N. and Y.G. conception and design of research; S.N. and A.D. performed experiments; S.N., A.D., and Y.G. analyzed data; S.N. and Y.G. interpreted results of experiments; S.N. and A.D. prepared figures; S.N. drafted manuscript; A.D. and Y.G. edited and revised manuscript; Y.G. approved final version of manuscript.

REFERENCES

Arieli A, Sterkin A, Grinvald A, Aertsen A. Dynamics of ongoing activity: explanation of the large variability in evoked cortical responses. *Science* 273: 1868–1871, 1996.

Asadollahi A, Mysore SP, Knudsen EI. Rules of competitive stimulus selection in a cholinergic isthmic nucleus of the owl midbrain. *J Neurosci* 31: 6088–6097, 2011.

Bala AD, Spitzer MW, Takahashi TT. Auditory spatial acuity approximates the resolving power of space-specific neurons. *PLoS One* 2: e675, 2007.

Bala AD, Takahashi TT. Pupillary dilation response as an indicator of auditory discrimination in the barn owl. *J Comp Physiol A* 186: 425–434, 2000.

Barry RJ. Habituation of the orienting reflex and the development of preliminary process theory. *Neurobiol Learn Mem* 92: 235–242, 2009.

Benowitz LI, Karten HJ. Organization of the tectofugal visual pathway in the pigeon: a retrograde transport study. *J Comp Neurol* 167: 503–520, 1976.

Boehnke SE, Munoz DP. On the importance of the transient visual response in the superior colliculus. *Curr Opin Neurobiol* 18: 544–551, 2008.

Boly M, Balteau E, Schnakers C, Degueldre C, Moonen G, Luxen A, Phillips C, Peigneux P, Maquet P, Laureys S. Baseline brain activity fluctuations predict somatosensory perception in humans. *Proc Natl Acad Sci USA* 104: 12187–12192, 2007.

Bradley MM. Natural selective attention: orienting and emotion. *Psychophysiology* 46: 1–11, 2009.

Cohen YE, Miller GL, Knudsen EI. Forebrain pathway for auditory space processing in the barn owl. *J Neurophysiol* 79: 891–902, 1998.

du Lac S, Knudsen EI. Neural maps of head movement vector and speed in the optic tectum of the barn owl. *J Neurophysiol* 63: 131–146, 1990.

Engel AK, Singer W. Temporal binding and the neural correlates of sensory awareness. *Trends Cogn Sci* 5: 16–25, 2001.

Fecteau JH, Munoz DP. Salience, relevance, and firing: a priority map for target selection. *Trends Cogn Sci* 10: 382–390, 2006.

Felix D, Wu GY, Wang SR. GABA as an inhibitory transmitter in the pigeon isthmo-tectal pathway. *Neurosci Lett* 169: 212–214, 1994.

Fiser J, Chiu C, Weliky M. Small modulation of ongoing cortical dynamics by sensory input during natural vision. *Nature* 431: 573–578, 2004.

Fox MD, Raichle ME. Spontaneous fluctuations in brain activity observed with functional magnetic resonance imaging. *Nat Rev Neurosci* 8: 700–711, 2007.

Fox MD, Snyder AZ, Vincent JL, Corbetta M, Van Essen DC, Raichle ME. The human brain is intrinsically organized into dynamic, anticorrelated functional networks. *Proc Natl Acad Sci USA* 102: 9673–9678, 2005.

Fox MD, Snyder AZ, Vincent JL, Raichle ME. Intrinsic fluctuations within cortical systems account for intertrial variability in human behavior. *Neuron* 56: 171–184, 2007.

Frost BJ, Nakayama K. Single visual neurons code opposing motion independent of direction. *Science* 220: 744–745, 1983.

Gaither NS, Stein BE. Reptiles and mammals use similar sensory organizations in the midbrain. *Science* 205: 595–597, 1979.

Goddard CA, Sridharan D, Huguenard JR, Knudsen EI. Gamma oscillations are generated locally in an attention-related midbrain network. *Neuron* 73: 567–580, 2012.

Gutfreund Y. Stimulus-specific adaptation, habituation and change detection in the gaze control system. *Biol Cybern* 106: 657–668, 2012.

Gutfreund Y, Zheng W, Knudsen EI. Gated visual input to the central auditory system. *Science* 297: 1556–1559, 2002.

Hesselmann G, Kell CA, Eger E, Kleinschmidt A. Spontaneous local variations in ongoing neural activity bias perceptual decisions. *Proc Natl Acad Sci USA* 105: 10984–10989, 2008.

Hikosaka O, Takikawa Y, Kawagoe R. Role of the basal ganglia in the control of purposive saccadic eye movements. *Physiol Rev* 80: 953–978, 2000.

Huguenard JR, McCormick DA. Thalamic synchrony and dynamic regulation of global forebrain oscillations. *Trends Neurosci* 30: 350–356, 2007.

Knudsen EI. Auditory and visual maps of space in the optic tectum of the owl. *J Neurosci* 2: 1177–1194, 1982.

Knudsen EI. Fundamental components of attention. *Annu Rev Neurosci* 30: 57–78, 2007.

Knudsen EI. Control from below: the role of a midbrain network in spatial attention. *Eur J Neurosci* 33: 1961–1972, 2011.

Knudsen EI, Cohen YE, Masino T. Characterization of a forebrain gaze field in the archistriatum of the barn owl: microstimulation and anatomical connections. *J Neurosci* 15: 5139–5151, 1995.

Lai D, Brandt S, Luksch H, Wessel R. Recurrent antitopographic inhibition mediates competitive stimulus selection in an attention network. *J Neurophysiol* 105: 793–805, 2011.

Lampl I, Reichova I, Ferster D. Synchronous membrane potential fluctuations in neurons of the cat visual cortex. *Neuron* 22: 361–374, 1999.

Lewis CM, Lazar AE. Orienting towards ensembles: from single cells to neural populations. *J Neurosci* 33: 2–3, 2013.

Luksch H. Cytoarchitecture of the avian optic tectum: neuronal substrate for cellular computation. *Rev Neurosci* 14: 85–106, 2003.

Maczko KA, Knudsen PF, Knudsen EI. Auditory and visual space maps in the cholinergic nucleus isthmi pars parvocellularis of the barn owl. *J Neurosci* 26: 12799–12806, 2006.

Marin G, Salas C, Sentis E, Rojas X, Letelier JC, Mpodozis J. A cholinergic gating mechanism controlled by competitive interactions in the optic tectum of the pigeon. *J Neurosci* 27: 8112–8121, 2007.

Marin GJ, Duran E, Morales C, Gonzalez-Cabrera C, Sentis E, Mpodozis J, Letelier JC. Attentional capture? Synchronized feedback signals from the isthmi boost retinal signals to higher visual areas. *J Neurosci* 32: 1110–1122, 2012.

Masino T, Knudsen EI. Horizontal and vertical components of head movement are controlled by distinct neural circuits in the barn owl. *Nature* 345: 434–437, 1990.

McPeek RM, Keller EL. Deficits in saccade target selection after inactivation of superior colliculus. *Nat Neurosci* 7: 757–763, 2004.

Mysore SP, Asadollahi A, Knudsen EI. Global inhibition and stimulus competition in the owl optic tectum. *J Neurosci* 30: 1727–1738, 2010.

Mysore SP, Asadollahi A, Knudsen EI. Signaling of the strongest stimulus in the owl optic tectum. *J Neurosci* 31: 5186–5196, 2011.

Mysore SP, Knudsen EI. The role of a midbrain network in competitive stimulus selection. *Curr Opin Neurobiol* 21: 653–660, 2011.

Mysore SP, Knudsen EI. A shared inhibitory circuit for both exogenous and endogenous control of stimulus selection. *Nat Neurosci* 16: 473–478, 2013.

Naatanen R. The mismatch negativity: a powerful tool for cognitive neuroscience. *Ear Hear* 16: 6–18, 1995.

Netser S, Ohayon S, Gutfreund Y. Multiple manifestations of microstimulation in the optic tectum: eye movements, pupil dilations, and sensory priming. *J Neurophysiol* 104: 108–118, 2010.

Netser S, Zahar Y, Gutfreund Y. Stimulus-specific adaptation: can it be a neural correlate of behavioral habituation? *J Neurosci* 31: 17811–17820, 2011.

Neuenschwander S, Engel AK, Konig P, Singer W, Varela FJ. Synchronization of neuronal responses in the optic tectum of awake pigeons. *Vis Neurosci* 13: 575–584, 1996.

Nir Y, Hasson U, Levy I, Yeshurun Y, Malach R. Widespread functional connectivity and fMRI fluctuations in human visual cortex in the absence of visual stimulation. *Neuroimage* 30: 1313–1324, 2006.

Nir Y, Mukamel R, Dinstein I, Privman E, Harel M, Fisch L, Gelbard-Sagiv H, Kipervasser S, Andelman F, Neufeld MY, Kramer U, Arieli A, Fried I, Malach R. Interhemispheric correlations of slow spontaneous neuronal fluctuations revealed in human sensory cortex. *Nat Neurosci* 11: 1100–1108, 2008.

Olsen JF, Knudsen EI, Esterly SD. Neural maps of interaural time and intensity differences in the optic tectum of the barn owl. *J Neurosci* 9: 2591–2605, 1989.

Perez ML, Pena JL. Comparison of midbrain and thalamic space-specific neurons in barn owls. *J Neurophysiol* 95: 783–790, 2006.

Perez ML, Shanbhag SJ, Pena JL. Auditory spatial tuning at the crossroads of the midbrain and forebrain. *J Neurophysiol* 102: 1472–1482, 2009.

Raichle ME. Neuroscience. The brain's dark energy. *Science* 314: 1249–1250, 2006.

Rankin CH, Abrams T, Barry RJ, Bhatnagar S, Clayton DF, Colombo J, Coppola G, Geyer MA, Glanzman DL, Marsland S, McSweeney FK, Wilson DA, Wu CF, Thompson RF. Habituation revisited: an updated and revised description of the behavioral characteristics of habituation. *Neurobiol Learn Mem* 92: 135–138, 2009.

Reches A, Gutfreund Y. Stimulus-specific adaptations in the gaze control system of the barn owl. *J Neurosci* 28: 1523–1533, 2008.

Reches A, Gutfreund Y. Auditory and multisensory responses in the tectofugal pathway of the barn owl. *J Neurosci* 29: 9602–9613, 2009.

Reches A, Netser S, Gutfreund Y. Interactions between stimulus-specific adaptation and visual auditory integration in the forebrain of the barn owl. *J Neurosci* 30: 6991–6998, 2010.

Rodriguez E, George N, Lachaux JP, Martinerie J, Renault B, Varela FJ. Perception's shadow: long-distance synchronization of human brain activity. *Nature* 397: 430–433, 1999.

Sadaghiani S, Hesselmann G, Kleinschmidt A. Distributed and antagonistic contributions of ongoing activity fluctuations to auditory stimulus detection. *J Neurosci* 29: 13410–13417, 2009.

Shadlen MN, Britten KH, Newsome WT, Movshon JA. A computational analysis of the relationship between neuronal and behavioral responses to visual motion. *J Neurosci* 16: 1486–1510, 1996.

Shimizu T, Bowers AN. Visual circuits of the avian telencephalon: evolutionary implications. *Behav Brain Res* 98: 183–191, 1999.

Shimizu T, Karten HJ. The avian visual system and the evolution of the neocortex. In: *Vision, Brain, and Behavior in Birds*, edited by Zeigler HP, Bischof HJ. Cambridge, MA: MIT Press, 1993, p. 103–114.

Sokolov EN. Higher nervous functions; the orienting reflex. *Annu Rev Physiol* 25: 545–580, 1963.

Sorenson EM, Parkinson D, Dahl JL, Chiappinelli VA. Immunohistochemical localization of choline acetyltransferase in the chicken mesencephalon. *J Comp Neurol* 281: 641–657, 1989.

Sridharan D, Boahen K, Knudsen EI. Space coding by gamma oscillations in the barn owl optic tectum. *J Neurophysiol* 105: 2005–2017, 2011.

Stein BE, Meredith MA. *The Merging of the Senses*. Cambridge, MA: MIT Press, 1993.

Super H, van der Togt C, Spekreijse H, Lamme VA. Internal state of monkey primary visual cortex (V1) predicts figure-ground perception. *J Neurosci* 23: 3407–3414, 2003.

Thompson RF, Spencer WA. Habituation: a model phenomenon for the study of neuronal substrates of behavior. *Psychol Rev* 73: 16–43, 1966.

Tsodyks M, Kenet T, Grinvald A, Arieli A. Linking spontaneous activity of single cortical neurons and the underlying functional architecture. *Science* 286: 1943–1946, 1999.

Wagner H. Sound-localization deficits induced by lesions in the barn owl's auditory space map. *J Neurosci* 13: 371–386, 1993. [Erratum. *J Neurosci* 13 (Apr): following table of contents, 1993.]

Wang CA, Boehnke SE, White BJ, Munoz DP. Microstimulation of the monkey superior colliculus induces pupil dilation without evoking saccades. *J Neurosci* 32: 3629–3636, 2012.

Wang Y, Luksch H, Brecha NC, Karten HJ. Columnar projections from the cholinergic nucleus isthmi to the optic tectum in chicks (*Gallus gallus*): a possible substrate for synchronizing tectal channels. *J Comp Neurol* 494: 7–35, 2006.

Wang Y, Major DE, Karten HJ. Morphology and connections of nucleus isthmi pars magnocellularis in chicks (*Gallus gallus*). *J Comp Neurol* 469: 275–297, 2004.

Wathey JC, Pettigrew JD. Quantitative analysis of the retinal ganglion cell layer and optic nerve of the barn owl *Tyto alba*. *Brain Behav Evol* 33: 279–292, 1989.

Weinberger NM, Oleson TD, Ashe JH. Sensory system neural activity during habituation of the pupillary orienting reflex. *Behav Biol* 15: 283–301, 1975.

Winkowski DE, Knudsen EI. Top-down gain control of the auditory space map by gaze control circuitry in the barn owl. *Nature* 439: 336–339, 2006.

Winkowski DE, Knudsen EI. Top-down control of multimodal sensitivity in the barn owl optic tectum. *J Neurosci* 27: 13279–13291, 2007.

Woods EJ, Frost BJ. Adaptation and habituation characteristics of tectal neurons in the pigeon. *Exp Brain Res* 27: 347–354, 1977.

Zahar Y, Reches A, Gutfreund Y. Multisensory enhancement in the optic tectum of the barn owl: spike count and spike timing. *J Neurophysiol* 101: 2380–2394, 2009.

Zanos TP, Mineault PJ, Pack CC. Removal of spurious correlations between spikes and local field potentials. *J Neurophysiol* 105: 474–486, 2011.